

RSC Advances



This is an *Accepted Manuscript*, which has been through the Royal Society of Chemistry peer review process and has been accepted for publication.

Accepted Manuscripts are published online shortly after acceptance, before technical editing, formatting and proof reading. Using this free service, authors can make their results available to the community, in citable form, before we publish the edited article. This *Accepted Manuscript* will be replaced by the edited, formatted and paginated article as soon as this is available.

You can find more information about *Accepted Manuscripts* in the [Information for Authors](#).

Please note that technical editing may introduce minor changes to the text and/or graphics, which may alter content. The journal's standard [Terms & Conditions](#) and the [Ethical guidelines](#) still apply. In no event shall the Royal Society of Chemistry be held responsible for any errors or omissions in this *Accepted Manuscript* or any consequences arising from the use of any information it contains.



Highly percolated poly(vinyl alcohol) and bacterial nanocellulose synthesized in-situ by physical-crosslinking: Exploiting polymer synergies for biomedical nanocomposites

Received 00th January 20xx,
Accepted 00th January 20xx

DOI: 10.1039/x0xx00000x

www.rsc.org/

C. Castro^{*a}, R. Zuluaga^a, O. J. Rojas^b, I. Filpponen^b, H. Orelma^b, M. Londoño^c, S. Betancourt^a, P. Gañán^a

Bacterial cellulose (BC) grown from a culture medium in the presence of water-soluble poly(vinyl alcohol) (PVA) produced an assemblage that was used as precursor for the synthesis of biocompatible nanocomposites. Physical crosslinking via cyclic freezing and thawing of the formed hydrogel facilitated retention of PVA matrix upon composite separation and purification. The composites displayed a porous architecture within the PVA matrix and an excellent compressive strength as a result of the synergism between BC and PVA. BC largely improved the thermo-mechanical performance as well as moisture and dimensional stability of the systems while PVA imparted optical transparency and extensibility. Compared to the respective reference sample (BC-free material), elastic modulus increments of 40, 98 and 510 % were measured for PVA-based nanocomposites loaded with BC at 10, 20 and 30% levels, respectively. Likewise, the corresponding strength at break were 30, 77 and 104 % higher. The results indicate an exceptional reinforcing effect endowed by the three-dimensional network structure that was formed in-situ upon BC biosynthesis in the presence of PVA and also suggest a large percolation within the matrix. BC is relatively inexpensive, can produce scaffolds of given shapes and with high strength and acts as an excellent reinforcing element that promotes cell proliferation. Taken these properties together, BC and BC/PVA composites are promising materials in biomedical engineering.

formation that links PVA chains by hydrogen bonds forming a network^{1,2,4}.

1 Introduction

Polyvinyl alcohol (PVA) is a material with an excellent biosafety profile, which has been successfully used in many pharmaceutical and biomedical applications. However, PVA already extensive list of uses finds some limitations in terms of its mechanical performance. Therefore, some nanoscale modifications have been proposed to enhance macroscopic properties¹. These include crosslinking to form hydrogels that are suitable for drug delivery, contact lenses, corneal implants and substitutes of skin, tendons, ligaments, cartilage and bones². Broadly, hydrogels are three-dimensional networks formed from homopolymers, copolymers or hydrophilic macromers and can form insoluble structures upon chemical (via bifunctional agents, etc.) or physical crosslinking³. Residual chemical crosslinking agents in PVA hydrogels may be difficult to remove and may not be desirable in biomedical and pharmaceutical applications⁴. Therefore, physical gelation and solidification methods are suitable alternatives. For example, repeated cycles of freezing and thawing can result in crystal

The freeze-thaw process can produce materials with a wide range of mechanical properties, however, in many cases it may be insufficient to fulfill the load bearing demands of replacements for damaged or diseased tissues². Thus, biocompatible reinforcing elements of both organic and inorganic nature are highly desirable. It is not surprising that cellulose has been generally considered as an alternative reinforcement⁵⁻¹¹. The main advantages of cellulose, as in fibers, include their low cost, high availability, biodegradability, high stiffness, low density and good mechanical properties¹². Among the different sources of cellulose, bacterial cellulose (BC) has gained considerable interest for biomedical applications and has been used as artificial skin, in wound treatment, as an artificial replacement for blood vessels and meniscus implants, among others^{13,14}. BC has been used as a reinforcement in biomedical composites¹⁵⁻¹⁹. Recently, cellulose-PVA composites have been reported²⁰⁻²⁶. However, the strong tendency of BC to aggregate makes homogenization and incorporation in PVA matrices difficult. In our previous work, we have shown that it is possible to develop composites of PVA reinforced with BC during synthesis by *Gluconacetobacter medellinensis* bacteria, in which the BC reinforcement is homogeneously distributed in the composite and the matrix is chemically crosslinked²⁷. In such process bacterial cellulose nanofibril network is generated by the

^a School of Engineering, Universidad Pontificia Bolivariana, Circular 1 # 70-01, Medellín, Colombia. Address here.

^b Biobased Colloids and Materials Group (BiCMat), School of Chemical Technology, Aalto University, FI-00076 Aalto, Finland

^c † Biomaterials Laboratory, Department of Biomedical Engineering, Engineering School of Antioquia —EIA—, CES University, Sabaneta, Colombia.

microorganism within the PVA matrix and enables the design of new, high-performance materials. However, as discussed before, the development of biomedical materials demands the elimination of crosslinkers to avoid possible toxicity in the body. Therefore, here we take advantage of the remarkable reinforcement effect of BC to synthesize nanocomposites with polyvinyl alcohol via (physical) cross-linking, which not only prevents PVA losses during purification but enhances the properties of the system to make it suitable for biomedical applications.

2 Materials and methods

Pre-conditioning of the microbial strain

The recently discovered *Gluconacetobacter* strain used in this study was isolated from a pellicle of homemade vinegar^{28,29}. The purified bacterium was incubated in a static Hestrin-Schramm culture medium (HS) containing 2 w/v% glucose, 0.5 w/v% peptone, 0.5 w/v% yeast extract, 0.27 w/v% Na₂HPO₄, adjusted to pH 3.5 by citric acid and autoclaved at 121 °C.

In situ production of PVA/BC nanocomposites

Poly(vinyl alcohol) (Sigma-Aldrich, Saint Louis, MO) with reported molecular mass of 146-186 kDa and 98-99% hydrolysis degree was added to the HS medium under stirring at 90 °C to obtain aqueous solutions of 0, 2.5, 5 and 10 wt% PVA concentrations. The modified HS media was inoculated with 10 v/v% of the preconditioned inoculum, and statically incubated for 8 days at 28 °C. The collected pellicles were subjected to 6 cycles of freezing and thawing between -20 and 20 °C with a rate of freezing and thawing of 0.1 °C/min and a holding time of 6 h, following the procedure implemented by Wan et al.³⁰. Pellicles linked physically were then washed with distilled water, immersed during 14 h in 5 wt% aqueous KOH solution and finally rinsed until pH 7 to remove any bacteria and residual components from the culture media.

Six sample batches were prepared for each PVA concentration. Three of the samples were physically crosslinked and three were used as reference to determine gravimetrically the amount of cellulose in the nanocomposites. Control samples of PVA (in the absence of BC) were also prepared following the same procedure used for the manufacture of the PVA/BC nanocomposites. A schematic diagram summarizing the manufacture procedure is provided in Figure 1. The composite and reference samples are referred thereafter as "PVA/BC X(Y)" and "PVA_Y", respectively, where "X" refers to the BC content or loading in the obtained nanocomposite (on a dry basis) and Y, added as reference, indicates the PVA concentration used in the precursor culture medium (see Table 1).

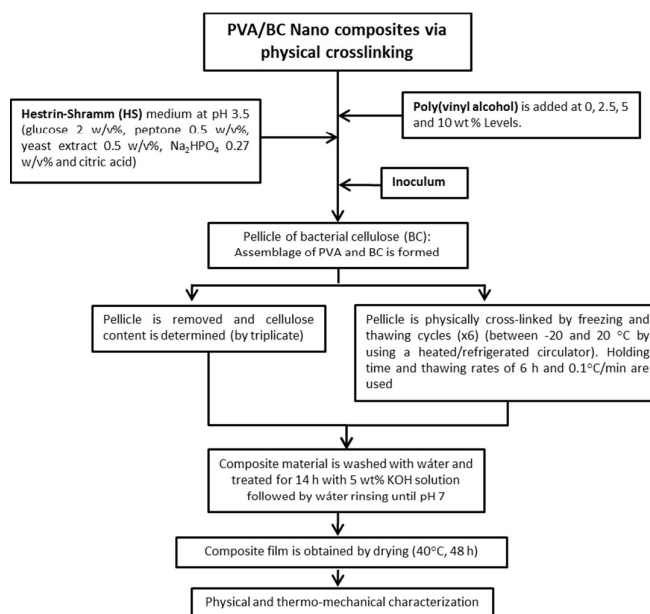


Figure 1. Block diagram with the steps used to synthesize PVA nanocomposites loaded with BC upon in situ biosynthesis from *Gluconacetobacter* bacterium. The control or reference samples were obtained by using the same procedure but no inoculum was added to the system.

PVA/BC nanocomposite characterization

Scanning electron microscopy (SEM, Jeol JSM 5910 LV operated at 10 kV) was used to image the fracture surfaces of dry nanocomposites deformed in tension and the surface of lyophilized nanocomposites. Before SEM analyses all specimens were coated with gold/palladium using an ion sputter coater for 5 min.

Attenuated total reflection Fourier transform infrared spectroscopy (ATR-FT-IR) was used to identify main chemical features of the PVA/BC nanocomposites. Before the measurement, the nanocomposites were dried for 2 h at 40 °C to precondition the test samples. ATR-FT-IR spectra were recorded on a Nicolet 6700 spectrophotometer in the 4000-400 cm⁻¹ range ATR with a diamond crystal. The spectra were recorded with a resolution of 4 cm⁻¹ and an accumulation of 64 scans.

Nanocomposite	BC loading in the composite, wt% (dry basis)	PVA concentration in the initial culture medium, wt%	Reference sample
PVA/BC 10(10)	10 ± 0.6	10	PVA10
PVA/BC 20(5)	20 ± 0.2	5	PVA5
PVA/BC 30(2.5)	30 ± 0.3	2.5	PVA2.5

Table 1. PVA/BC nanocomposites nomenclature and respective composition, listed with increased BC % loading based on the total mass of the solid material (PVA+BC). The figures in parenthesis represent the PVA concentration used in the precursor culture medium.

Mechanical properties

Tensile strength was measured for dry specimens (dry condition after purification step were 40 °C, 48 h), cut according to ASTM D-1708 standard and preconditioned at 24 °C and 75% RH. The strength at break and elastic modulus were determined with an Instron Instrument according to ASTM D-882 using a load cell of 200 N at 5 mm/min and 22 mm grip distance.

Dynamic mechanical analysis (DMA) with humidity control was carried out with a Q 800 DMA (TA Instruments) equipped with a humidity chamber. Oscillatory measurements (1 Hz frequency) were performed at 23 °C using 5.3 mm x 12 mm strips cut from the physical linked nanocomposites and reference samples. Samples were loaded to the chamber and conditioned in 0 %RH for 240 min. Thereafter, two humidity cycles of varying %RH (between 0 and 90 %) were applied using 480 min as equilibrium time. The data was collected every 2 seconds until reaching equilibrium.

Samples films were cut into disks (25 mm diameter) that were conditioned in distilled water at room temperature for 24 h to hydrate samples (gel state). The compression behavior in gel state was evaluated on a TA Rheometer (parallel plate geometry with a diameter of 20 mm). An initial strain of 10% was used to ensure that the measurement was carried out in the elastic region.

Thermal properties

The thermal degradation behavior of the dry composite samples was determined by thermogravimetry (TGA, Mettler Toledo). The TGA apparatus was flushed with nitrogen atmosphere and 10 mg samples were used. Each specimen was heated from room temperature to 800 °C at a rate of 10 °C/min. Differential scanning calorimetry (DSC, Mettler Toledo) was used to acquire thermograms under N₂ flow. Samples (5 mg) were placed in hermetically closed DSC crucibles and heated from -40 °C to 250 °C at 10 °C/min to erase the thermal history, after which they were cooled to -40 °C at 10 °C/min. The second heat scan was conducted from -40 °C to 250 °C at 10 °C/min and the glass transition temperature (*T_g*) was taken as the inflection point of the specific heat increment at the glass-rubber transition while the melting temperature (*T_m*) was taken as the peak temperature of the melting endotherm. Before the tests all specimens were cut in equal circles of 2 mm in diameter and dried at 100 °C for 2 h.

Two crystallinity parameters were determined from eq 1 and 2, from the sample weight, *X_c* and from the amount of matrix material in the composite, *X_p*. In the calculation ΔHm° is taken as the heat of fusion for 100% crystalline PVA, assumed to be 161.6 Jg⁻¹ and *w* is the weight fraction of PVA matrix material in the composite³¹.

(1)

$$X_c = \Delta Hm / \Delta Hm^\circ$$

(2)

$$X_p = X_c / w$$

3 Results and discussion

PVA/BC nanocomposites were produced during the biosynthesis of cellulose in static conditions by bacteria of the genus *Gluconacetobacter*. After fermentation, PVA added to the culture medium was physically cross-linked with the reinforcing BC fibrils by freeze/thawing cycles to improve bonding and prevent losses of the PVA matrix during material washing and purification. Table 1 includes the composition of the final nanocomposites obtained from different PVA and BC ratios. The precursor PVA concentration in the culture media was initially 2.5, 5 and 10 wt% resulting in nanocomposites with BC weight percent based on total dry mass that was determined to be 30, 20 and 10 wt%, respectively. Therefore, the composites were manufactured with PVA as main component and BC as minor, reinforcing phase. A decrease in BC production was observed in the presence of large amounts of PVA in the culture medium, mainly owing to the increased viscosity of the medium, which hindered the transfer of microorganisms to the surface where it consumes oxygen for metabolism. Additional factors that may prevent BC production include the possibility of PVA acting as a barrier to oxygen diffusion through the medium as also was observed in previous work using in situ PVA chemical crosslinking²⁷.

Figure 2 includes images of the "PVA2.5" sample (the matrix without BC, see nomenclature in Table 1) as well as PVA/BC 30(2.5) composite as well as a film of neat BC. The PVA matrix (PVA2.5) is transparent, which is in contrast to the case of the BC film, which is translucent. When the BC is synthesized in the culture medium in the presence of PVA, the obtained composite material (PVA/BC 30(2.5), Figure 1) remains transparent, even at such high BC loading (30 wt%). This is due to the good homogenization of the BC in the PVA matrix during its synthesis and their strong interaction and interfacial adhesion. The resultant optical characteristics of the nanocomposites are an advantage in applications that demand high transparency, as in the development of artificial corneas, which also requires high mechanical strength¹⁷.

Figure 3 includes ATR-FT-IR spectra of PVA, BC and PVA/BC nanocomposites after the respective washing and purification procedure (Figure 1). Nanocomposite spectra (Figures 3b-d) include the characteristic PVA matrix bands (Figure 3a). The characteristic cellulose signals of C-O-C pyranose ring skeletal vibration at 1060 and 1030 cm⁻¹ (indicated by the solid lines) are observed in all of PVA/BC nanocomposites (Figure 3e). At increased cellulose content the intensity of the band also increases in the spectra of the composites. Others characteristic bands of cellulose are not distinguishable in the nanocomposite, mainly because of the relative low amount of BC loading relative to PVA, and band overlapping at given wavelength.



Figure 2. Photographs of samples consisting of PVA 2.5 reference (without bacterial cell) (a), PVA/BC 30(2.5) nanocomposite (b) and a film of neat bacterial cellulose (c). See Table 1 for nomenclature

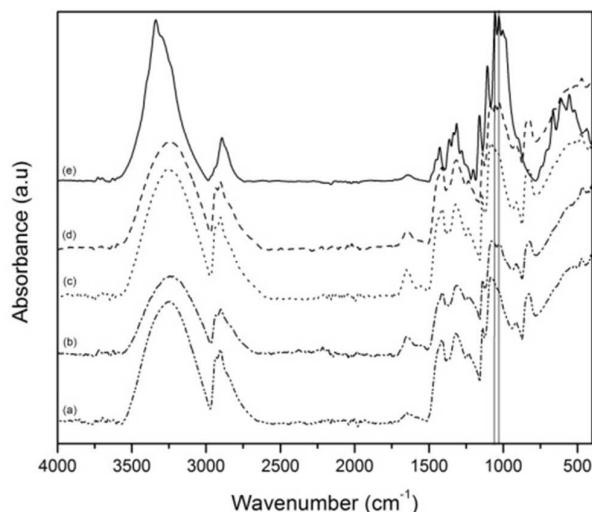


Figure 3. ATR-FT-IR spectra of crosslinked nanocomposites containing different BC loadings: (a) PVA, (b) PVA/BC 30(2.5), (c) PVA/BC 20(5), (d) PVA/BC 10(10) and (e) Bacterial cellulose.

Tensile behavior of PVA and PVA/BC composite films are included in Figure 4. Under the same testing conditions, the reference PVA matrices display a highly elastic behavior. The presence of BC in the nanocomposite changes such behavior as the stiffness of the nanocomposites increased drastically with BC loading. It is observed that both Young's modulus (YM) and strength at break increase markedly with the reinforcing BC: relative to the control sample (in absence of BC), increases in YM of 40, 98 and 510 % are determined for nanocomposites with 10, 20 and 30% BC loadings, respectively. The corresponding increase in tensile strength at break are 30, 77 and 104%. The results indicate an exceptional reinforcing effect by the three-dimensional network structure formed by the BC upon biosynthesis in the presence of PVA and also suggest a large percolation within the matrix^{27,32}. Remarkably, this improvement in mechanical performance have not been reported before for PVA composites reinforced with various cellulosic elements^{20-23,33-35}.

This behavior is closely tied to the nanocomposite manufacturing method, wherein microorganism bioengineering facilitates an intimate contact between the reinforcing phase and the matrix for a maximum percolation.

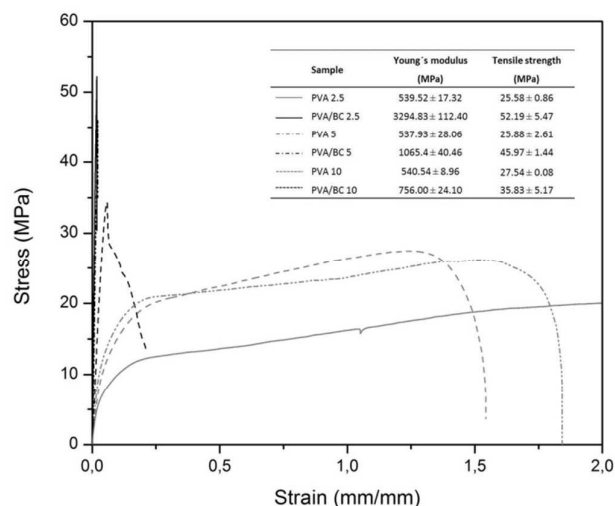


Figure 4. Stress-strain behavior observed in tensile tests for PVA/BC composites (black profiles) and for the respective matrix or reference (indicated in grey profiles) synthesized by physical crosslinking.

SEM images of the fractured surfaces of BC, PVA reference films (prepared from 10 wt% aqueous solution, PVA10 and the nanocomposites (PVA/BC 10(10), PVA/BC 20(5) and PVA/BC 30(2.5), see also Table 1) are shown in Figure 5. Figure 5a shows a uniform fracture of PVA10 film with flow lines in the matrix indicating that the rupture was caused by a crack propagation on the smooth, brittle surface. The nanocomposite fractures show no evidence of agglomerates indicating that the BC ribbons were homogeneously distributed throughout the matrix (Figure 5c-e). Moreover, good compatibility between the reinforcing PVA and the BC matrix (good fiber-matrix bonding) is suggested by the absence of pull-out BC ribbons. Moreover, the typical delamination of BC films observed in Figure 5b is prevented in the nanocomposites even though some minor delamination (indicated by circles in Figure 5b) was noted to occur at high BC loading. In these latter conditions chemical crosslinking may be effective to control possible delamination^{27, 36,37}. Undulation of inner layers shown in Figure 5d could be associated to an anisotropic behavior as consequence of biosynthesis that should be studied broadly.

Figure 6 shows the TG and DTG curves for nanocomposites and their respective references. The first change between 40 and 150 °C corresponds to the evaporation of absorbed and linked water incorporated during the preconditioning at 75% RH of all samples. A second transition presented only in the case of PVA reference films is due to structural degradation. The third loss weight transition occurred between 350 and 400 °C corresponding to the maximum degradation temperature in all samples, namely, upon charring. The onset and maximum temperature of thermal degradation increase with the BC loading in the network, indicating that it endows composites with higher thermal stability, possibly due to the excellent dispersion and compatibility of BC and PVA matrix.

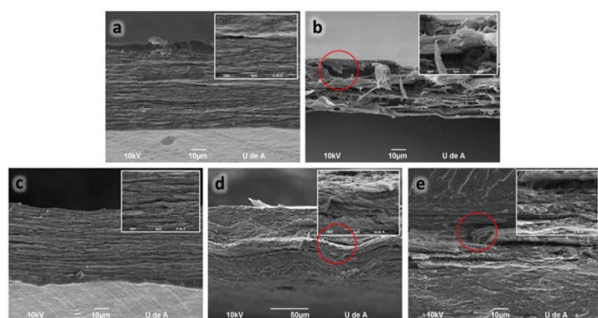


Figure 5. SEM images of tensile fracture surface of materials: (a) physical linked PVA10, (b) bacterial cellulose and physical linked (c) PVA/BC 10(10), (d) PVA/BC 20(5) and (e) PVA/BC 30(2.5) nanocomposites.

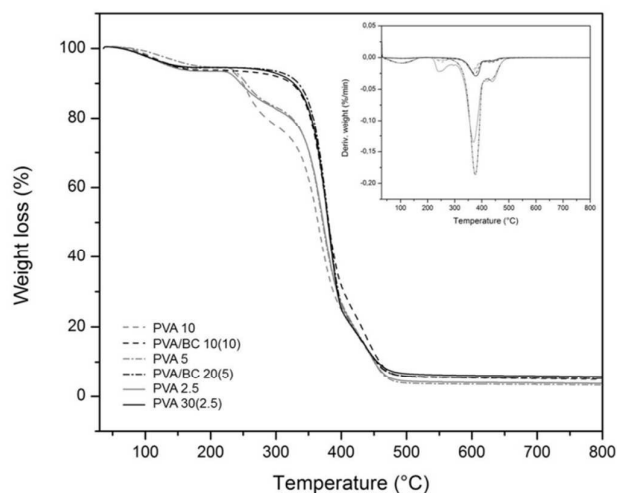


Figure 6. Thermal degradation profiles of physically crosslinked PVA/BC composites. The black profiles correspond to the nanocomposite while the gray profiles correspond to the respective matrix or reference sample.

The thermal behavior of the samples was also studied by DSC (Table 2). The glass transition T_g and melting T_m temperatures were shifted to higher values with BC loading in the nanocomposites. This is, also explained by the strong interactions and high compatibility between the reinforcing phase and the matrix. Likewise, the network formed by nanoscale ribbons decreases the mobility of PVA chains at the interface³¹. The degree of crystallinity of the material (X_c) and the crystallinity of the matrix in the nanocomposite (X_p) was calculated from ΔH data as presented in Table 2. A slight increase in the crystallinity of the PVA was observed in the nanocomposite with 10 wt% of BC, but at higher BC loading the crystallinity decreased. This argues for the fact that with 10 wt% BC loading, cellulose ribbons promote crystal formation (nucleating agent) but above this concentration the reinforcing restricts the ability of the matrix to form large crystalline domains³¹.

To assess changes in the mechanical behavior of the nanocomposites when subjected to humid environments, the films were exposed to humidity cycles between 0 and 90% RH in a DMA (see Figure 7). The changes seen in the storage

modulus were accompanied by changes in the deformation of the material as the relative humidity of the surrounding environment was changed. Figure 7a shows that in all samples the modulus decreased with increasing humidity, as expected, due to the plasticizing effect of water. However, compared to BC-free films, more limited changes were observed for the BC-loaded nanocomposites (less sensitivity to air humidity). Thus, BC improves the mechanical stability.

Similarly, changes in the dimensions of the materials were observed with moisture gain. Figure 7b shows an increase in the dimensions of the system as the percentage of relative humidity increases. As for the case of the elastic module, greater dimensional stability is presented in nanocomposites with higher BC content. Dimensional stability provided by the BC network is consistent with the fact that the cellulose component restricts the flow of the PVA chains³⁸.

Sample	T_g (°C)	T_m (°C)	ΔH (Jg ⁻¹)	X_c (%)	X_p (%)
PVA10	76.2	224.7	69.7	0.43	0.43
PVA/BC 10(10)	79.7	236.4	68.3	0.42	0.47
PVA5	69.2	225.3	73.3	0.45	0.45
PVA/BC 20(5)	78.8	230.6	48.1	0.30	0.37
PVA2.5	63.5	228.1	59.3	0.37	0.37
PVA/BC 30(2.5)	84.2	229.8	43.9	0.23	0.33

Table 2. Thermal transitions and crystallinity (*) of matrices and cross-linked nanocomposites reinforced at various BC loadings.

(*) $X_c = \Delta H_m / \Delta H_m^\circ$ and $X_p = X_c / w$; with $\Delta H_m^\circ = 161.6$ Jg⁻¹ (heat of fusion for 100% crystalline PVA³¹). w is the weight fraction of polymeric matrix material in the composite.

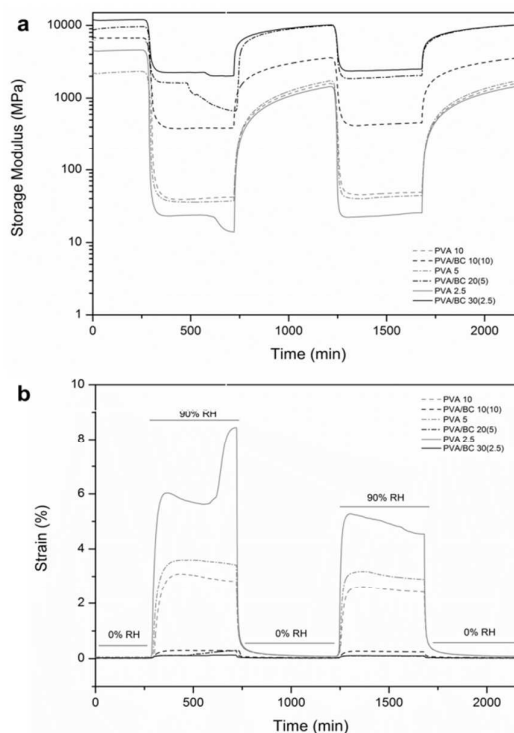


Figure 7. Variation of the storage modulus (a) and strain (b) of nanocomposites (black profiles) and respective control (grey profiles) after two humidity cycles between 0 and 90% RH at room temperature.

The storage modulus and strain of the PVA matrix and the respective nanocomposites fully and reversibly recovered after undergoing the humidity cycles. This elastic behavior is not affected by dehydration and hydration of the specimens. Consequently, the net effect of cellulose network coupled with strong reinforcing-matrix interactions restricted the movement of PVA chains, providing mechanical and dimensional stability to the composite.

Materials in a hydrated state (hydrogel) were also examined, the surface of nanocomposites and their respective reference samples were examined by SEM. Images taken of hydrogels surface are presented in Figure 8. The lyophilized materials exhibited a porous architecture, which was strongly influenced by the presence of the BC network. Moreover, the surface in PVA references change from an open to a closed cell structure in the nanocomposites.

At the same magnification BC appears as a network, which is formed by the cellulose nanoribbons. In the nanocomposites these cellulose ribbons and PVA chains are associated through hydrogen bond during the freezing and thawing process, leading to the formation of compact structure walls between the pores²⁸. This behavior is maintained throughout and within the material. Overall, the observed features are relevant to biomedical applications where porous surfaces are necessary for cell proliferation in tissue formation and the controlled release of drugs^{39,40}.

The mechanical behavior of the material in a hydrated state was evaluated by compression tests in the elastic range. The compressive elastic modulus was measured for all samples and the results are presented in Table 3. It has been recorded that the membranes of BC in a hydrated state have good tensile behavior, but very poor compressive strength. Similarly, PVA has limitations as far as its mechanical behavior under compression^{14,41-43}. These findings are in agreement with our results for BC and PVA (PVA2.5, PVA5 and PVA10) (Table 3). The PVA/BC 10(10) composite shows a compressive elastic modulus of 2.7 MPa, which is more than 48 times than that of BC (0.058 MPa), and almost ten times than for the PVA10 reference (0.270 MPa). The evidence that the module of the nanocomposite is much higher than that of the constituents is a remarkable example of the synergy between PVA and BC upon physical crosslinking. Interestingly, this behavior resembles observations in natural cartilage^{44,45}. It is then conceivable that BC plays a role such like that of collagen fibers while PVA acts as a proteoglycan matrix. Overall, the presented results show the promise of the obtained materials for applications such as cartilage replacement.

Figure 9a shows the rheological response of the viscoelastic materials at different frequencies. For all samples, the storage modulus has a weak dependence on the frequency between 0.05 to 100 rad/s, suggesting that the samples have high elasticity. In this frequency range, the nanocomposites had higher storage modulus than their respective components. This observation points to the reinforcing effect of the BC network and thus the improved mechanical response of the nanocomposites, as was the case for dry films. Similarly Figure 9b shows the dependence of the strain of the storage modulus at a given frequency. At 1 Hz the storage modulus for the nanocomposite materials increased due to reinforcing effect of BC network. The module in the reference materials was not affected by changes in strain up to 1%, which implies a reversible behavior. However, such reversibility was less pronounced in nanocomposites with high BC loading: thus, it can be concluded that the BC network limits the elastic behavior of the composite²⁵. The strong interactions between BC and PVA in the wet and dry state and the resulting composite with superior thermo-mechanical performance is illustrated schematically in Figure 10, where a highly percolated network and extensive hydrogen bonding are observed as key features.

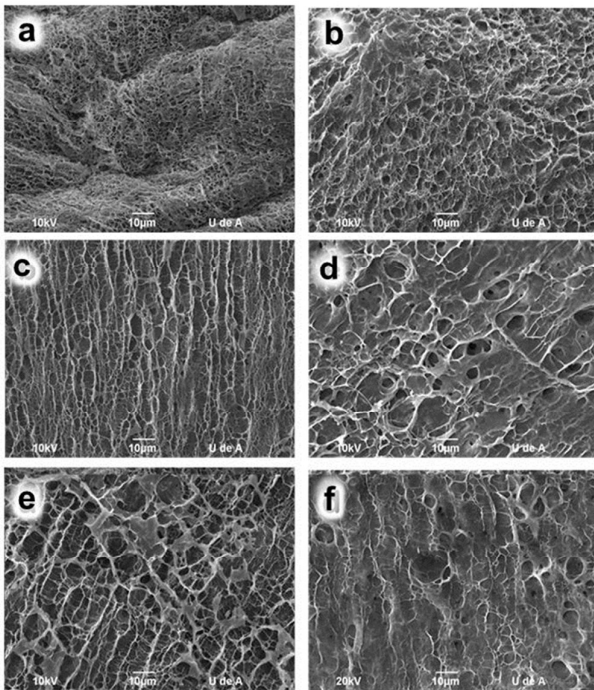


Figure 8. SEM images of physical linked surface of reference materials and respective PVA/BC nanocomposite: (a) PVA10, (b) PVA/BC10(10), (c) PVA5, (d) PVA/BC20(5), (e) PVA 2.5 and (f) PVA/BC 30(2.5).

Sample	Modulus (MPa)
BC	0.058± 0.002
PVA10	0.270± 0.013
PVA/BC 10(10)	2.754± 0.193
PVA5	0.076± 0.006
PVA/BC 20(5)	2.100± 0.168
PVA2.5	0.023± 0.001
PVA/BC 30(2.5)	0.039± 0.002

Table 3. Compression modulus of physical cross-linked nanocomposites and respective references measured in the hydrated state

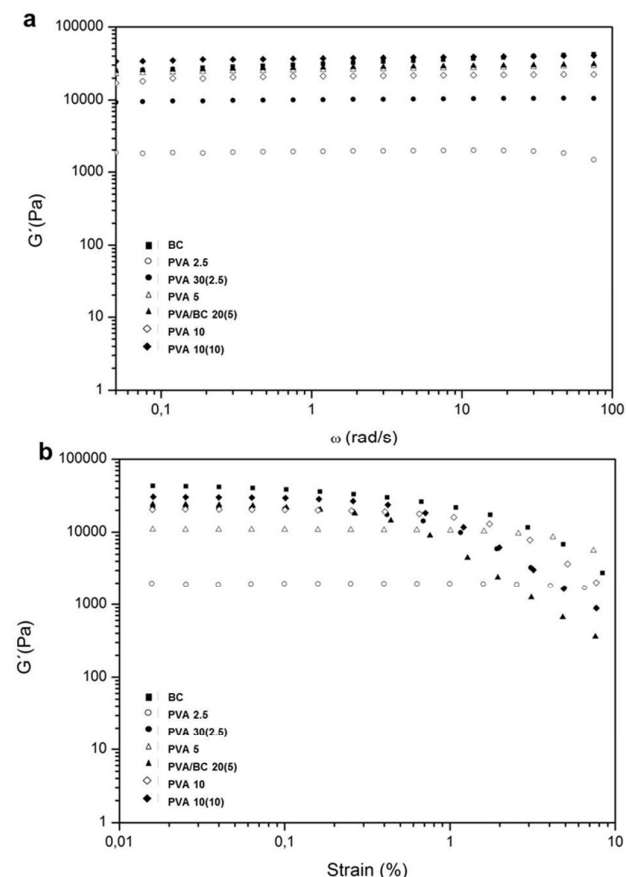


Figure 9. Storage modulus variation as a function of frequency at 1% strain (a) and as a function of strain at 1 Hz frequency (b) for the physical cross-linked nanocomposites and their references tested in the hydrated or wet state.

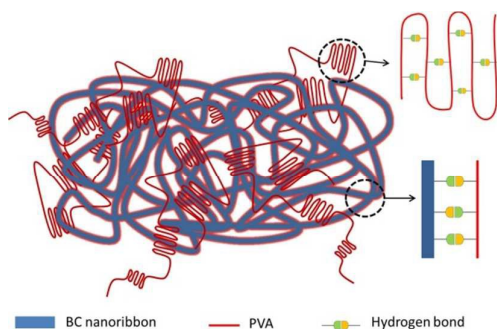


Figure 10. Schematic rendition (not to scale) of the possible interactions between PVA and BC upon physical cross-linking, mainly via mechanical entanglement and hydrogen bonding interactions.

Conclusions

PVA/BC nanocomposites were produced in situ in the presence of bacterial cellulose biosynthesis from *Gluconacetobacter* strains. In order to avoid matrix losses during processing steps, the materials were physically cross-linked by freezing and thawing cycles. Nanocomposites with different physical and

mechanical characteristics were obtained and included a BC network distributed homogeneously throughout the matrix forming a percolating cluster. Likewise, due to high affinity between the reinforcement and the matrix, the presence of the BC network in the nanocomposite provides an outstanding and synergistic mechanical performance as well as improved thermal and dimensional stability with moisture, all while maintaining the optical characteristics of the matrix. The nanocomposite characteristics in hydrated state were assessed and a highly porous architecture of the PVA matrix was observed to change depending on BC loading. The compressive mechanical behavior of the nanocomposite (hydrogels) showed distinctively the synergistic effect between BC and the PVA matrix, their combination improved the elastic modulus of the synthesized materials.

From rheological tests it was also found that the presence of the BC network increases the shear module in the nanocomposites, but limits their viscoelasticity in wet state. Overall, the results indicate that by using the proposed synthesis method it is possible to design biocompatible PVA/BC nanocomposites with a variety of physical-mechanical features that are of relevance in biomedical applications such as cell and tissue regeneration, controlled drug release and as substitutes of cartilage, corneas, veins and arteries.

Corresponding Author

*Corresponding author: E-mail: cristina.castro@upb.edu.co; phone: + 57-4-4488388

Author Contributions

The manuscript was written through contributions of all authors. All authors have given approval to the final version of the manuscript.

Acknowledgements

Arja Vesterinen (Aalto University) is greatly appreciated for her assistance in dynamic mechanical measurements. Colombia's COLCIENCIAS and SENA are acknowledged for financial support and travel stipend to Aalto University (CC). OJR acknowledges support by the Academy of Finland's Centres of Excellence Programme under the project "Molecular Engineering of Biosynthetic Hybrid Materials Research" (HYBER).

References

- 1 M-H. Alves, B.E. Jensen, A.A. Smith and A.N. Zelikin, *Macromol. Biosci.*, 2011, 11, 1293-1313.
- 2 J.A. Stammen, S. Williams, D.N. Ku and R.E. Gulberg, *Biomaterials*, 2001, 22, 799-806.
- 3 B.V. Slaughter, S.S. Khurshid, O.Z. Fisher, A. Khademhosseini and N.A. Peppas, *Adv Mater*, 2009, 21, 3307-3329.

- 4 C.M. Hassan and N.A. Peppas, *Adv Polym Sci*, 2000,153, 37-65.
- 5 J.S. Jeong, J.S. Moon, S.Y. Jeon, J.H. Park, P.S. Alegaonkar and J.B. Yoo, *Thin Solid Films*, 2007, 515, 5136-5141.
- 6 K.K.H. Wong, M. Zinke-Allmang, J.L. Hutter, S. Hrapovic, J.H.T. Luong and W. Wan, *Carbon*, 2009, 47, 2571-2578.
- 7 K.H. Hong, *Polym Eng Sci*, 2007, 47, 43-49.
- 8 H.M. Ji, H.W. Lee, M.R. Karim, I.W. Cheong, E.A. Bae, T.H. Kim, M.S. Islam, B.C. Ji and J.H. Yeum, *Colloid Polym Sci*, 2009, 287, 751-758.
- 9 C. Shao, H.Y. Kim, J. Gong, B. Ding, D.R. Lee and S.J. Park, *Mater Lett*, 2003, 57, 1579-1584.
- 10 E. Madeiros, L. Mattoso, R. Offeman, D. Wood and W.J. Orts, *Can J Chemistry*, 2008, 86,590-599
- 11 J. Junkasem, R. Rujiravanit and P. Supaphol, *Nanotechnology*, 2006, 17,4519-4528
- 12 A.K. Bledzki and J. Gassan, *Prog Polym Sci*, 2009, 24, 221-274
- 13 J.D. Fontana, A.M. De Sousa, C.K. Fontana, I.L. Torriani, J.C. Moreschi, B.J. Gallotti, S.J. De Sousa, G.P. Narcisco, J.A. Bichara and L.F. Farah, *Appl Biochem Biotechnol*, 1990, 24, 253-264.
- 14 A. Bodin, S. Concaro, M. Brittberg and P. Gatenholm, *J Tissue Eng Regen Med*, 2007, 1:406-408
- 15 L.E. Millon, C.J. Oates and W. Wan, *J Biomed Mater Res B*, 2009, 90B, 922-929.
- 16 Y.Z. Wan, L. Hong, S.R. Jia, Y. Huang, Y. Zhu, Y.L. Wang and H.J. Jiang, *Compos Sci Technol*, 2006, 66,1825-1832
- 17 J. Wang, C. Gao, Y. Zhang and Y. Wan, *Mater Sci Eng C*, 2010, 30, 214-218
- 18 L. Hong, Y.L. Wang, S.R. Jia, Y. Huang, C. Gao and Y.Z. , *Mater Lett*, 2006, 60, 1710-1713.
- 19 Z. Cai and J. Kim, *Cellulose*, 2011,17,83-91.
- 20 W. Zhang, X. Yang, C. Li, M. Liang, C. Lu and Y. Deng , *Carbohydr Polym*, 2011, 83, 257-263.
- 21 J. Lu, T. Wang and L.T. Drzal, *Composite Part A*, 2008, 39:738-746.
- 22 M. Roohani, Y. Habibi, N.M. Belgasem, G. Ebrahim, A.N. Karimi and A. Dufresne, *Eur Polym J*, 2008, 22:2489-2498
- 23 Q. Cheng, S. Wang and T. Rials, *Composites Part A*, 2009, 10, 218-224.
- 24 J. Leitner, B. Hinterstoisser, M. Wastyn, J. Keckes, W. Gindl, *Cellulose*, 2007, 14, 419-425.
- 25 C. Chang, A. Lue and L. Zhang. *Macromol Chem Phys*, 2008, 209, 1266-1273.
- 26 E.H. Qua, P.R. Hornsby, H.S.S. Sharma, G. Lyons and R.D. McCall, *J Appl Polym Sci*, 2009, 113, 2238-2247
- 27 C. Castro, A. Vesterinen, R. Zuluaga, G. Caro, I. Filpponen, O. Rojas, G. Kortaberria and P. Gañán, *Cellulose*, 2014, 21,1745-1756
- 28 C. Castro, I. Cleenwerck, J. Trcek, R. Zuluaga, P. De Vos, G. Caro, R. Aguirre,J-L. Putaux and P. Gañán , *Int J Syst Evol Microbiol*, 2013,63, 1119-1125.
- 29 C. Castro, R. Zuluaga, A.L. Álvarez, J-L. Putaux, G. Caro, O. Rojas, I. Mondragon, P. Gañán, *Carbohydr. Polym.*, 2012, 89, 1033-1037.
- 30 W.K. Wan , G. Campbell , Z.F. Zhang , A.J. Hui and D.R. Boughner, *J Biomed Mater Res B*, 2002, 63, 854-61.
- 31 M. Roohani, Y. Habibi, N.M. Belgasem, G. Ebrahim, A.N. Karimi and A. Dufresne, *Eur Polym J*, 2008, 22, 2489-2498
- 32 M.A.S.A. Samir, F. Alloin and A. Dufresne, *Biomacromolecules*, 2005, 6:612-626.
- 33 T. Zimmermann, E. Pöhler and T. Geiger, *Adv Eng Mater*, 2004, 6, 754-761.
- 34 S-Y. Lee, D.M. Mohan, I-A. Kang, G-H. Doh, S. Lee and S.O. Han, *Fiber Polym*, 2009, 10, 77-82.
- 35 K. Qiu and A. Netravali, *J Mater Sci.*, 2012, 47, 6066-6075.
- 36 F. Quero, M. Nogi, K-Y. Lee, G. Vanden Poel, A. Bismarck, A. Mantalaris, H. Yano and S.J. Eichhorn, *ACS Appl. Mater. Inter.*, 2011, 3, 490-499.
- 37 F. Quero, M. Nogi, K-Y. Lee, H. Yano, K. Abdulsalami, S.M. Holmes, B.H. Sakakini and S.J. Eichhorn, *ACS Appl. Mater. Inter.*, 2010, 2,321-330.
- 38 M.S. Peresin, Y. Habibi, A.H. Vesterinen, O.J. Rojas, J.J. Pawlak and J.V. Seppala, *Biomacromolecules*, 2010, 11 ,2471-2477.
- 39 V.I. Lozinsky and F.M. Plieva, *Enzyme Microb Technol.*, 1998, 23, 227-242
- 40 L.E. Millon and W.K. Wan, *J Biomed Mater Res B*, 2006, 79B, 245-253.
- 41 A. Nakayama, A. Kakugo, J.P. Gong, Y. Osada, M. Takai, T. Erata and S. Kawano, *Adv Funct Mater*, 2004, 14, 1124-1128.
- 42 Y. Hahiwara, A. Putra, A. Kakugo, H. Furukawa and J.P. Gong, *Cellulose*, 2009, 17, 93-101.
- 43 L.E. Millon, C.J. Oates and W. Wan, *J Biomed Mater Res B*, 2009, 90B, 922-929.
- 44 G.E. Kempson (1979) Mechanical properties of articular cartilage. In: Freeman AR (Ed) *Adult Articular Cartilage*. Pitman Medical,Turnbridge Wells, pp. 333-413.
- 45 L.A. Setton, D.M. Elliott and V.C. Mow, *OsteoarthR Cartilag*, 1999, 7, 2-14